Impact of Wind Turbine Generator Technologies and Frequency Controls on the Stable Operation of Medium Voltage Islanded Microgrids

Dominik Willenberg*, Alexander Winkens, Philipp Linnartz
Institute for High Voltage Equipment and Grids, Digitalization and Power Economics
RWTH Aachen University
Aachen, Germany
*d.willenberg@iaew.rwth-aachen.de

***Abstract*—In islanded microgrids, wind turbine generators have a significant impact on the power balance requiring a stability-supporting behavior. Therefore, the impact of technological characteristics and frequency control approaches of wind turbine generators needs to be identified. In this paper, the impact of wind turbine generator technologies and frequency controls in existing medium voltage islanded microgrids is evaluated. Different technologies and frequency-dependent active power adjustment control approaches are analyzed regarding the impact on a stable islanded microgrid operation. Based on the conducted investigations, the impact of the technology of wind turbine generators on the stable operation of islanded microgrids differs only marginally. The utilization of a virtual inertia concept without deadband hysteresis in medium voltage islanded microgrids positively affects the stable operation. Moreover, in case of multiple units, the diversity of technology and frequency control parameterization leads to a more stable islanded microgrid operation.**

***Index Terms*-- Doubly-fed asynchronous machine, full-scale converter, islanding, microgrids, wind power generation.**

I. INTRODUCTION

The increased penetration of distributed generation (DG) units in the electrical power grid, especially on low (LV) and medium voltage (MV) levels, may result in a local generation surplus [1]. In case of an interruption of power supply, this development offers the opportunity for a temporary islanded microgrid (IM) operation at the distribution grid level. When a DG unit with grid-forming and blackstart capability (e.g. a synchronous generator in a combined heat and power plant (CHP)) is present, the IM is able to contribute to the overlaying grid restoration process [2]. Due to a lack of conventional power plants and a subsequent lack of inertia in IMs, sudden power changes may lead to larger deviations in frequency in comparison to parallel grid operation [3]. Due their power ratings, wind turbine generators (WTGs), such as doubly fed induction generators (DFIGs) or full-scale converter WTGs (FCWTGs), have a significant impact on the power balance compared to single PV or CHP units. Therefore, a stability supporting dynamic behavior of WTGs is essential for a stable grid operation [4]-[6].

In Germany, the MV grid code (GC) determines that DG units in the MV level have to provide ancillary services, such as the adaption of active power infeed depending on the grid frequency, which may influence the grid frequency after a contingency [7]. In grid-connected operation mode of the microgrid, WTGs typically operate at their maximum power point (MPP) feeding in the maximum available power at the current wind speed [8]. Therefore, the active power cannot be increased in under frequency situations. According to the GC, when WTGs operate at MPP, this frequency dependent active power adjustment (FDAPA) concept can be reduced to a frequency dependent active power reduction (FDAPR) strategy in over frequency situations. If WTGs are operated at MPP in MV IMs, the FDAPR may not be sufficient to ensure a stable operation of the IM during under frequency situations.

Due to the comparably large share of active power infeed of WTGs at MPP, the influence of the technology (DFIG or FCWTG) and the frequency control of WTGs on the stable operation of MV IMs needs to be investigated [4]. So far, the impact of the integration of DG units, particularly WTGs, on the operation of IMs in existing distribution grid structures is demonstrated in several research projects (e.g. in [9]). However, mostly a specific real grid topology is used. Moreover, a dominant grid-forming unit is typically present, which is able to supply the maximum power demand [9], [10]. Usually these conditions are not provided by existing distribution grid structures, which are not explicitly designed for islanded operation. For this reason, this paper investigates the contribution of WTGs to a stable operation of MV IMs formed by a comparably lower-scale synchronous generator. The investigation is focused on the suitability of the frequency support concepts given by the GC in case of IM operation. First, the applicability of FDAPR is evaluated. Second, a Virtual Inertia (VI) based control scheme for under frequency situations is proposed and expanded in order to reduce potentially critical frequency peaks. Based on that, the impact of the WTG

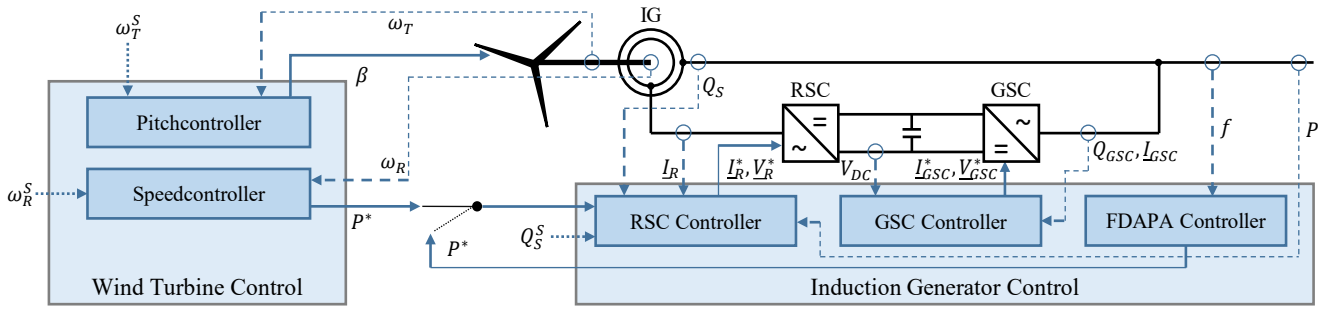

Figure 1. Control structure of the WTG DFIG

technology on the grid frequency is analyzed. The introduced FDAPA controls are verified based on a 3-bus-IM using time-domain simulations (TDSs) for analyzing the impact onto the stable operation of MV IMs. Finally, a modified CIGRE MV benchmark grid is implemented and TDSs are performed in order to evaluate the mitigation of disturbances by parameter variation.

II. Modeling Approach

The execution of RMS TDSs requires dynamic models (DMs) of the different DG units as well as DMs of the IM itself. To ensure a continuous IM operation, a generation unit with grid-forming capability is needed. In this paper, a CHP is considered for this purpose, which is coupled to the grid by a synchronous generator (SG). The consumer loads are implemented as ZIP load models. Moreover, the two WTG technologies, DFIG and FCWTG, are modelled and extended using three types of FDAPA controls, which are deduced from the behavior demanded by the German GC:

1. FDAPR in case of generation surplus (over frequency)
2. VI-based FDAPA for improvement of frequency stability in under frequency situations
3. VI-based FDAPA with frequency support for a longer timeframe and partially defined electric power output during rotor speed recovery

The simulations are carried out in the symmetric RMS TDS environment "MatPAT" (Matlab-based Power System Analysis Toolbox) using an implicit-explicit solver [11].

A. Component models

1) Synchronous generator

The SG simulation model is based on the fundamental machine equations: stator and rotor voltage equations and the related flux equations [12]. In order to be able to consider the detailed transient behavior of the SG, a 6th order model is implemented [13]. In addition, the generic IEEE DC1A model is used as excitation system [14]. The aim of FDAPA defined in the GC is to return the frequency inside the deadband between 49.8 Hz and 50.2 Hz. For this reason, the grid forming SG is equipped with a secondary controller. In the dynamic model, this is achieved by adding an isochronous control to the IEEEG1 governor model [15].

2) Wind turbine generators

The two most common technologies for WTGs are FCWTG and DFIG WTGs. When the microgrid is in grid-connected mode WTGs are controlled using a maximum power point tracking (MPPT) algorithm feeding their maximum available active power into the grid [8]. In IMs, this condition does not have to be fulfilled because of a potential wind power generation surplus compared to the demand. However, this situation is assumed to be less critical regarding the frequency stability because of the possibility of a permanent increase of the active power infeed during under frequency situations. Thus, the dynamic WTG models focus on operation in MPP.

a) Doubly fed induction generators

WTGs based on DFIGs are coupled to the grid by the stator windings of the induction generator (IG) in parallel to a converter, which controls the rotor currents of the machine [8]. For the purposes of this paper the model is expanded by an interface to adjust the active power set point P^* in order to include the FDAPA control. The fundamental principle and control scheme of the DM are presented in Fig. 1. All variables with a superscript 'S' indicate values taken from the steady-state operating point (OP) while those with an index '*' indicate reference values. In contrast to the FCWTG model, the mechanical part has to be included because of the direct coupling of the DFIG stator windings to the grid [8]. The control of rotor speed ω_R is realized by the speed controller using the active power fed into the grid P as control variable. The comparably slower pitch controller is assumed to solely be able to reduce the mechanical power extracted from wind due to the MPPT operation. Therefore, focusing on the short term dynamics, it is used as a speed limiter. It should be noted that the model differentiates between turbine speed ω_T and the rotor speed ω_R of the IG by including mechanical damping and stiffness of the shaft. However, for the considerations of this paper, this effect is negligible.

The IG is modelled by a third-order model using the flux equations [16]. The rotor-side-converter (RSC) sets the rotor current $\underline{I}_R$ and voltage $\underline{V}_R$ to control the total active and reactive power fed into the grid to their reference values P^* and Q_S^S [17]. The grid-side converter (GSC) keeps the DC link voltage V_{DC} constant and sets the reactive power flow through the converter branch Q_{GSC} to zero. As for the RSC, this is achieved by acting on the AC-side converter current $\underline{I}_{GSC}$ and voltage $\underline{V}_{GSC}$ [16]. An additional controller is added for the

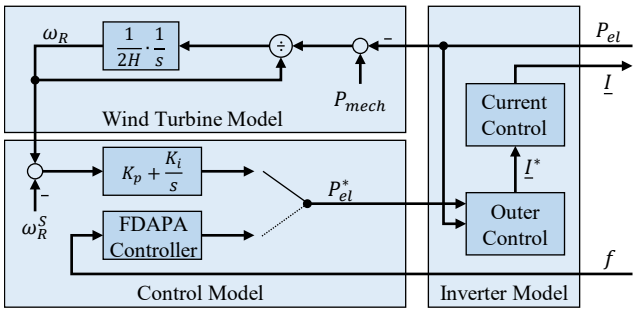

Figure 2. Dynamic model of the Full-Scale Converter WTG

implementation of FDAPA concepts, which calculates an active power reference P^* depending on the measured grid frequency f. In case of a grid frequency outside the deadband, this reference imposes the active power set point given by the speed controller. Hence, after the FDAPA controller is switched off, the rotor speed returns to its initial value and the speed controller dominates the control behavior again. The event of switching is determined by the chosen FDAPA strategy, frequency and rotor speed.

b) Full-scale converter WTGs

The FCWTG is represented by a generic, manufacturer independent dynamic inverter model introduced in [18]. On the grid connected AC side, the inverter is modelled as a controllable current source, which is powered by a constant voltage source on the DC side. In contrast to [18], instead of controlling the rotational energy using a P controller, the reduction of the rotor speed ω_R to its initial value ω_R^S after an operation in FDAPA-mode is realized by a PI rotor speed controller [18]. Thus, the comparability to the concept implemented in the DFIG DM is ensured. The overall scheme of the FCWTG model is presented in Fig. 2. The current rotor speed is calculated assuming that the difference between the mechanical power P_{mech} extracted from the wind and the electrical power P_{el} fed into the grid changes the rotational energy of the turbine and is described by the equation (1)

$$\frac{d\omega_R}{dt} = \frac{1}{2H}\cdot\frac{P_{mech} - P_{el}}{\omega_R} \tag{1}$$

with H representing the total inertia of all rotating parts. As for the DFIG, the electrical power reference P_{el}^* is calculated either by the PI speed controller parameterized by the gains K_p and K_i or by the FDAPA controller depending on the current operation mode. The time of switching is depending on the FDAPA strategy, the frequency and the rotor speed. Finally, the inverter sets P_{el}^* by acting on the current $\underline{I}$ which is fed into the grid.

3) Load

For the representation of the load, a ZIP load model including an additional frequency dependency is used [13]. Due to the different behavior of residential and industrial areas, the overall load is parameterized partly residential and industrial, which results in a load including partly constant power, constant current and constant impedance factors. The evaluated events triggering frequency deviations are modelled by switching of a constant power load model.

4) Electricity grid

The resistance, reactance and susceptance of the MV lines are modelled via the standard pi equivalent circuit model. This way, a constant admittance matrix is constructed, which allows a continuous calculation of the power flow during the dynamic simulation. The results of a prior power flow calculation serve as initial OP and input for the dynamic simulation [12]. The grid frequency is independent of the location and defined to be proportional to the rotational speed of the grid-forming SG since no further synchronous rotating mass is considered in the simulations.

B. Modeling of FDAPA controls for WTGs

The guidelines for the FDAPA characteristic in German MV grids are shown in Fig. 3. When the grid frequency exceeds the deadband between 49.8 Hz and 50.2 Hz, DG units which are not directly connected to the grid by a SG, have to adapt their active power output according to the FDAPA characteristic as long as primary energy supply or technical limitations allow the operation at the respective set point. Equation (2) shows the calculation of the droop value s according to the German MV GC:

$$s = \left|\frac{\Delta f}{50\ Hz}\cdot\frac{P_{ref}}{\Delta P}\right| \tag{2}$$

where ΔP indicates the change of active power due to the frequency deviation, P_{ref} is defined as the stationary active power output before leaving the deadband and Δf represents the frequency deviation from the threshold of the deadband. The droop value can be chosen by the system operator in between 2 % and 12 %; s = 5 % is set as default value. For a frequency higher than 51.5 Hz or lower than 47.5 Hz, DG units are allowed to disconnect from the grid. Since the active power infeed of the DG units is needed to supply the load, the IM is assumed to be unstable, respectively.

1) FDAPR

The FDAPR only reduces active power infeed during over frequency situations as presented on the right side of Fig. 3. As the mechanical power initially remains constant, the wind turbine starts to accelerate. By using the pitch controller as speed limiter, the power extracted from the wind can be reduced and the rotor speed can be controlled to its steady-state value. Consequently, FDAPR operation is possible over a long period of time.

2) Virtual Inertia (VI)

In IMs with low synchronously coupled inertia and a significant amount of wind power generation, frequency support by WTGs in under frequency situations becomes important, even if it is not demanded by the GC for WTGs when operating in MPP. Considering that, a sole FDAPR control is not sufficient. For the increase of active power of WTGs using MPPT, the VI strategy, i.e. the extraction of rotational energy from the rotor of a WTG followed by a phase of feeding this energy back to the rotor, is already identified as an option [5], [18], [19]. VI opens the possibility of FDAPA in under and

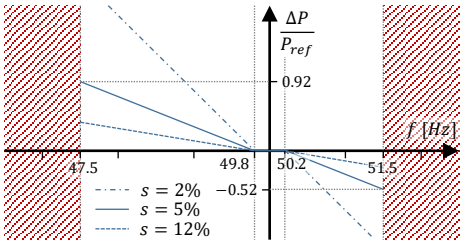

Figure 3. FDAPA characteristic according to German MV GC [7]

over frequency situations including the complete droop characteristic for a limited amount of time. However, the maximum extraction of rotational energy from the rotor of a WTG is set to $\Delta E_{\mathrm{rot}} = 2\,\%$. When the frequency reaches the deadband after the frequency has exceeded the deadband or the rotor speed reduces below a certain level, the WTG will decrease its active power infeed to a value lower than the initial value in steady state in order to accelerate the turbine to its original speed. Thus, a second frequency peak, in the following "speed recovery peak" (SRP), will occur during this speed recovery mode (SRM) [5].

3) VI with deadband hysteresis (DBH)

A smooth transition of active power infeed between the grid-supporting mode and the SRM can reduce the SRP and thus stabilize the grid [5]. Due to the sudden switch from FDAPA control to the PI speed controller, this is not given for the previously presented strategy. For this reason, an expanded VI controller, which smoothens the additional active power demand of the WTG, is implemented and tested regarding its applicability in WTG-dominated IMs. The FDAPA behavior demanded by the GC is expanded by a hysteresis loop, as depicted in Fig. 4. After reaching the frequency value 49.8 Hz again, the active power set point decreases further along the extension of the droop characteristic leading to an acceleration of the rotor speed. At the frequency f_{lim}, the speed controller is activated in order to return to MPP operation without any control deviation. Depending on the regained rotor speed, the PI controller is then expected to cause a lower SRP [5].

III. Case Studies

Based on a three-bus MV IM, the impact of the technology and the FDAPA strategies onto the stable operation of MV IMs is evaluated (Fig. 5). In the following, the behavior of two WTGs in a modified CIGRE MV benchmark grid is investigated regarding mitigation of disturbances by parameter variation of the respective DG units. All case studies are carried out by applying a positive or negative load step at $t = 1$s, which can represent a sudden DG outage or load disconnection. Furthermore, the average wind speed is assumed to be constant at 10 m/s during the dynamic simulation. Higher wind speeds are not considered to avoid the activation of the pitch control during MPPT operation. In case of higher wind speeds, the pitch control would adjust the rotor blades so that the WTG still feeds its nominal power into the grid. Lower wind speeds lead to a reduced amount of stored rotational energy, so that the maximal contribution of FDAPA controls cannot be

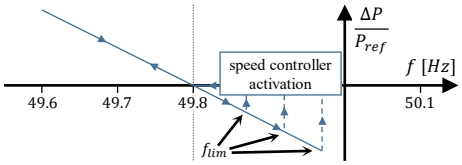

Figure 4. Addition of deadband hysteresis based on German MV GC [7]

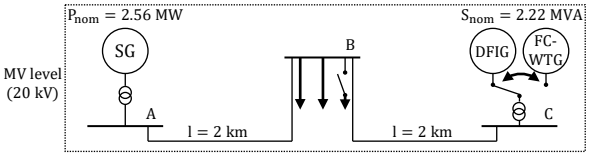

Figure 5. 3-bus MV IM topology

demonstrated. Therefore, additional active power infeed demanded by the grid could either be provided by the WTG only to a small extent because of WTG component limitations (lower wind speeds leading to a quadratic reduction of rotational energy) or any rotor speed drop could be eliminated by shortly increasing the mechanical power of the turbine (higher wind speeds). In this case, either the investigated concepts can be applied only in a strongly reduced number of scenarios or the frequency stability is expected to be less critical due to a missing SRP, respectively [5].

First, the presented FDAPA strategies are validated and evaluated using the three-bus MV IM (see Fig. 5). The busses A and B as well as B and C are linked by a MV cable with a length of 2 km. At bus A, the grid-forming SG with a nominal active power of 2.56 MW is connected. The load is modeled as half industrial and half residential at bus B, and is equivalent to total active power infeed of SG and WTGs before the applied load step for the different case studies. Furthermore, any load change event is applied at bus B. At bus C, either a DFIG WTG or a FCWTG is connected with a nominal apparent power of 2.22 MVA. This allows identifying technological differences influencing the dynamic behavior and the suitability of the FDAPA concepts. All simulations are carried out at different OPs of the WTGs and the SG. For the evaluation of the impact of parameter variation of multiple WTGs and their controls, the CIGRE European MV benchmark grid is used, which represents a close to reality MV German or European distribution grid [20]. The IM consists of two main feeders, which are split into three sub-feeders that can be meshed by switches connecting the ends of the feeders. The structure can be interpreted as the MV distribution grid of a small town. Therefore, a WTG is placed outside the city at busses 1 and 12 each while the CHP-driven SG is placed at bus 3 within the settled area. However, the comparably large loads at node 1 and 12 are not taken into account. The steady-state power flow, which is used as base for the dynamic simulations, is defined for a high load (3.8 MW) scenario with a significant active power infeed by two DFIGs of 1.6 MW each [20]. In order to identify mitigation of disturbances, the WTG technology and control strategy is varied. Furthermore, slight changes

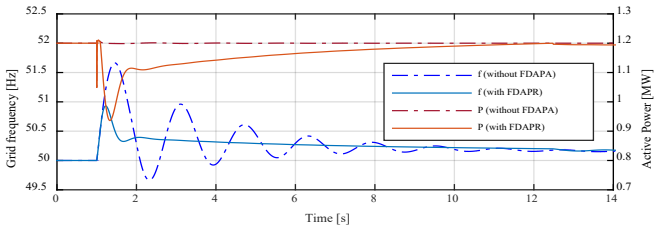

Figure 6. Frequency and Active Power using FDAPR when performing a load step of -0.3 MW at $t = 1$ s

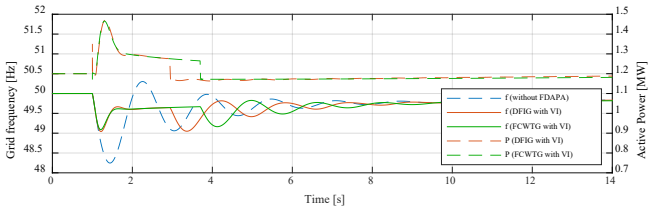

Figure 7. Frequency and Active Power using VI when performing a load step of 0.3 MW at $t = 1$ s

of different control parameters are applied to the WTGs. No additional DG units, e.g. PV units, are considered in order to exclude external influences on the dynamic behavior of the WTGs. This way, only the impact of the WTG technology and control strategies is determined.

IV. Simulation Results

A. *Validation and analysis of FDAPA strategies*

1) FDAPR

In order to validate the applicability of FDAPA the grid frequency and the active power infeed of a DFIG using either-FDAPR or no FDAPA control are shown over time in Fig. 6. The simulation is carried out on the 3-bus IM with a steady-state infeed of 1.2 MW of the SG and the DFIG each. At t =1 s, a decrease of the load by 0.3 MW is applied. The results show that FDAPR control can reduce the first frequency peak by about 47 % from 51.7 to 50.9 Hz. Thus, a frequency higher than the allowed limitation of 51.5 Hz is avoided. For this purpose, the active power infeed of the DFIG is temporarily reduced by up to 0.26 MW. Furthermore, due to its fast control of electrical output power, the DFIG with FDAPR suppresses further frequency oscillations caused by the governing system of the CHP-driven SG, which can be observed for the DFIG without FDAPA. At around $t = 11$ s after the decrease of the load, the frequency deadband of $f = 50.2$ Hz is reached again. Thus, FDAPA-based concepts as VI can also be promising in under frequency situations.

2) Virtual Inertia

The VI strategy is introduced at the same steady-state OP as the FDAPR, but with an increase of the load of 0.3 MW. The resulting frequency and active power infeed for FCWTG and DFIG are depicted in Fig. 7. By using VI, the first frequency dip can be reduced from 48.3 Hz to 49 Hz for DFIG and to 49.1 Hz for FCWTG. In contrast to FDAPR, the expected SRP occurs at $t = 3.4$ s for DFIG and $t = 4.1$ s for

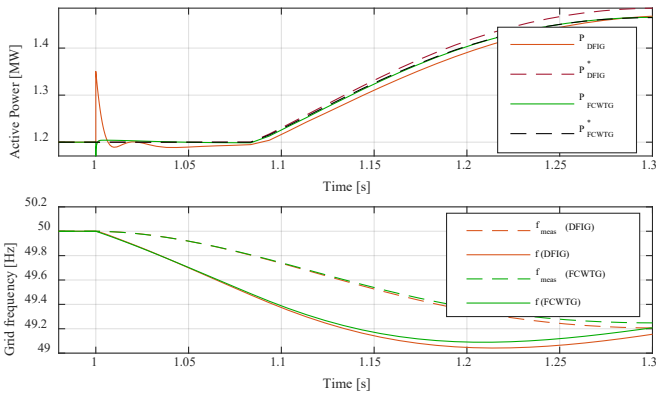

Figure 8. Active power and grid frequency of WTG technologies after load step of 0.3 MW at $t = 1$ s

FCWTG, respectively. At that time, the active power infeed decreases rapidly to a value smaller than in steady state. It should be noted that the SRP reaches a level comparable to the first frequency peak after the load step event. This is due to the parameterization and the choice of a PI speed controller. However, a smaller peak for the cost of a longer speed recovery time might not be reasonable in IMs due to the higher probability of frequency deviations compared to parallel grid operation. Concluding, VI enables a separation of one critical frequency dip into two minor peaks for both DFIG and FCWTG. Despite an equal parameterization, DFIG and FCWTG switch from FDAPA to SRM at different points in time. This is due to the negligence of ohmic losses and speed dependence of the extracted power from the wind in the FCWTG model. Thus, the DFIG model reaches the maximum rotational energy deviation of 2 % earlier than the FCWTG. Independent of the modeling, technological differences between the WTG types can be identified based on the behavior in the first 300 ms after the load step, which is presented in Fig. 8. Immediately after the load step, the DFIG provides an inertial response for around 10 ms by increasing its active power by up to 0.15 MW whereas for the FCWTG even a slight dip can be observed. However, the temporary increase of active power by the DFIG has a negligible effect on the grid frequency in comparison to the FCWTG. Furthermore, as the frequency exceeds the deadband, the active power output of the DFIG cannot follow its reference value (indicated with '*') as fast as the FCWTG. As a consequence, the

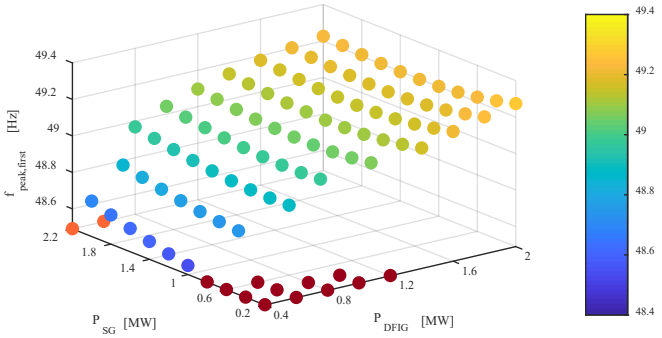

Figure 9. Frequency dip and stability depending on the OP of DFIG and SG

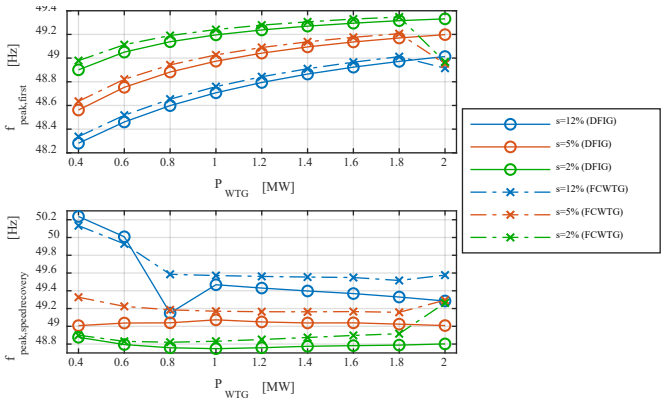

Figure 10. Effect of different droop values and the WTG technology on the first frequency peak and the speed-recovery peak

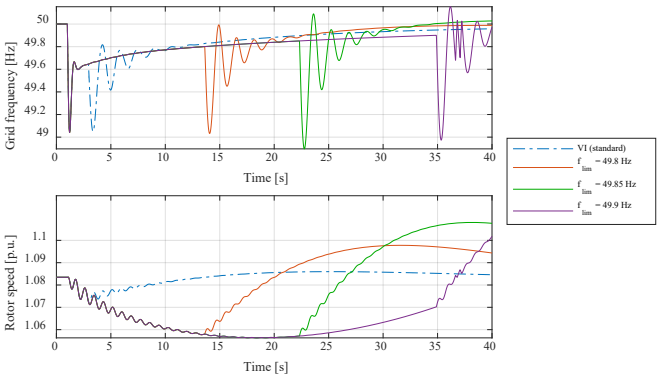

Figure 11. Frequency and rotor speed for VI with deadband hysteresis

frequency dip gets slightly more critical when using a DFIG.

Fig. 9 shows the dependence of the first frequency dip for a variation of the steady-state active power infeed OP of the SG and a DFIG in 0.2 MW steps. Furthermore, the red marked OPs indicate a control instability, i.e. the non-reaching of a new steady state, whereas the dark orange markers indicate an instability due to an exceedance of frequency limitations. It can be noticed that the first frequency peak is more sensitive to changes in active power of the DFIG than of the SG since the amount of active power WTGs provide to support the frequency is dependent on their steady-state infeed. For the reason of control instability, low OPs of the SG (P_{SG} < 1 MW) should be avoided, if the WTG cannot provide a high frequency supporting capability. On the other hand, high loading of the SG may lead to an exceedance of the frequency band since the SG is not able to increase its active power as dynamically when operating near the its nominal apparent power and limitations of its governor.

The impact of the droop value on the first peak and the SRP peak is shown in Fig. 10 for both WTG technologies with a SG infeed of 1.2 MW and an increase in load of 0.3 MW. The active power infeed of the WTG technologies is varied between 0.4 and 2 MW. Due to the stronger active power adaption at a lower droop value, the first frequency dip is less critical in this case. However, a lower droop value causes a faster return to SRM and results in a higher SRP. It should be noted that the SRP level can strongly be determined by the oscillating characteristic of the SG, if the WTG does only slightly contribute to frequency stability. This effect can be observed for s = 12 % and low steady-state infeed of the WTG.

3) VI with deadband hysteresis (DBH)

In order to investigate the impact of the DBH, the maximum allowed extracted rotational energy ΔE_{rot} is increased to 20 % to prevent switching to SRM before reaching the deadband, e.g. in Fig. 7. The frequency and the rotor speed of the DFIG WTG are displayed in Fig. 11 for the standard VI control as well as for the DBH with different f_{lim}. The DFIG WTG and the SG are feeding in 1.2 MW each. The applied load increase is 0.3 MW. In contrast to the expected effect, the SRP is neither reduced compared to the standard VI control nor when increasing the value of f_{lim}. A reason is that the rotor speed does not increase after reaching 49.8 Hz since the more detailed DFIG model is used, which considers the dependence between the mechanical power and the rotor speed. Thus, at 49.8 Hz the mechanical power is still smaller than the electrical power causing a further deceleration of the rotor. Furthermore, since a comparably long period of time is needed, the influence of the integral part of the speed controller becomes more significant. Hence, the SRP can become more critical even in case of similar rotor speed deviations. Concluding, the concept of DBH can be less suitable for the operation of an emergency IM due to the longer period of time the WTG needs to return to normal operation. Furthermore, depending on the implementation of the speed controllerof the WTG a more critical SRP may occur.

B. Mitigation of disturbances by parameter variation

In order to identify the impact of multiple WTGs with FDAPA control, a modified CIGRE benchmark MV grid is considered at a high load OP of 3.8 MW with a significant active power infeed by two DFIGs of 1.6 MW each. For both WTGs, the VI control without DBH is used. An increase in load of 0.3 MW is applied. Fig. 12 presents the grid frequency when increasing selected control parameters by 20 % identifying the influence of slightly different behaving WTGs. Furthermore, the yellow curve shows the frequency when one DFIG is replaced by a FCWTG. As a reference case, two DFIGs with the same standard parameterization are considered in the red curve. All additional parameter variations are applied on both WTGs. When changing parameters directly influencing the FDAPA control, e.g. the width of the frequency deadband, the inverse of the droop K_{FDAPA} or the allowed deviation of rotational energy ΔE_{rot}, the SRP splits into two less critical peaks compared to the use of the standard parameterization for both DFIGs. This is due to the maximum rotor speed deviation, which is achieved at different times for both DFIGs. The same situation applies to the replacement of one DFIG by a FCWTG due to their different dynamic modeling. It should be noted that this observation only holds true, if the activation of the SRM is caused by reaching the maximum rotor speed deviation but not by reaching the frequency deadband again. In this case, only a different width of the deadband can be expected to cause a similar behavior. In

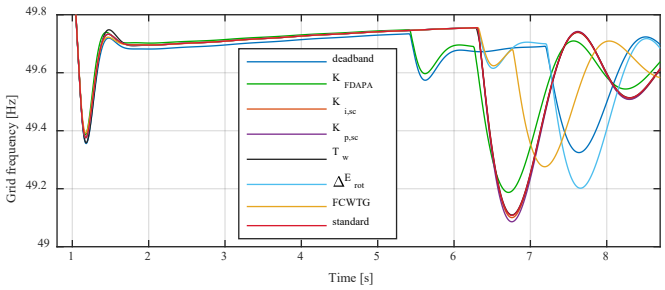

Figure 12. Grid frequency for two WTG considering parameter differences in a modified CIGRE benchmark MV grid

contrast to that, when changing WTG-related parameters, such as the gains of the speed controller $K_{p,sc}$ and $K_{i,sc}$ or the time constant T_w of the PT1-block used for the modeling of frequency measurement, the shape of the grid frequency does not change but only the peaks receive slight changes compared to the standard parameterization. Thus, in an IM with multiple WTGs a different parameterization of the VI-based FDAPA control as well as the existence of different WTG technologies or designs can improve the frequency behavior after an increase in load, since the SRP is split into several smaller peaks.

The obtained results solely base on TDSs. Although the modeling of the WTG technologies and control strategies shows the expected dynamic behavior, e.g. a stabilizing effect of the FDAPR control, individual manufacturer dependent dynamic WTG behavior may differ from the simulated dynamicbehavior and the contribution of the frequency support by WTGs may change. To include the individual dynamic behavior and to verify the obtained simulation results, it is necessary to perform laboratory and field studies in representative islanding scenarios in future work. This paper focusses on the evaluation of the impact and applicability of different FDAPA control strategies. Therefore, multiple scenarios have been simulated and analyzed (e.g. load and generation scenarios of the IM). Nevertheless, in order to operate the MV IM most durable, deviating operating and grid conditions, e.g. a change in wind speeds or IM conditions such as peak load fluctuations, need to be considered by an appropriate energy management system for the IM.

V. Conclusion and Outlook

The impact of WTG technologies and frequency controls on the stable operation of MV IMs is presented and discussed. Three different FDAPA control approaches for DFIG and FCWTGs - FDAPR according to current GC, VI-based FDAPA and VI-based FDAPA with DBH - are implemented in a RMS TDS environment. In addition, a 3-bus MV IM topology is set up with a grid-forming SG, a load and either a DFIG or a FCWTG connected to it. By applying a load step of -0.3 MW, the WTG with FDAPR control is able to reduce the frequency increase and to avoid an unstable IM operation. At MPP operation of the WTGs, VI-based concepts can be applied in order to improve the frequency behavior in MV IMs in case of a load increase. The VI-based FDAPA splits the occurring frequency peak into two smaller peaks due to the necessary SRP. By comparing the two WTG technologies, only a small impact on the reduction of the frequency peak can be noticed. However, the FCWTG is able to follow its active power reference value faster leading to a reduced first frequency dip. When varying the OPs of SG and DFIG, low OPs of the SG should be avoided, if the WTG cannot provide a high frequency supporting capability. An adjustment of the droop value leads to two main findings: a decrease of the droop coefficient leads to a larger active power adaption of the WTG and therefore significantly reduces the first frequency peak. However, the SRP increases due to a larger step in active power infeed of the WTG. When using the VI-based FDAPA with DBH, the expected smoothening effect onto the frequency in MV IMs does not occur. In contrast, an increased frequency limit at which the WTG should return to SRM leads to even larger SRPs in comparison with the VI-based FDAPA and is therefore not recommended for the operation in MV IMs. In a modified MV CIGRE benchmark grid, the mitigation of disturbances by parameter variation is evaluated. As base case, two WTGs with VI-based FDAPA without DBH and an active power infeed of 1.6 MW, a load of 3.8 MW and grid-forming SG covering the remaining demand are considered. In case of different WTG technologies, FCWTG and DFIG WTG and a different FDAPA control parameterization lead to a beneficial frequency behavior. The adjustment of WTG-related parameters (e.g. the gains for speed controllers or time constants for the frequency measurement) has almost no beneficial effect on the grid frequency. The results show that for future standardization of MV IMs and for a beneficial frequency behavior after contingencies, for WTGs at MPP the VI-based FDAPA control should be taken into consideration.

In future work the influence and interactions between WTGs and additional PV units or battery storage systems as well as dynamic load behavior need to be evaluated. Moreover, a combination with demand side management control strategy approaches is to be evaluated to enable a frequency supporting component behavior by generation and load.

VI. References

[1] “World Energy Outlook 2017”, International Energy Agency (IEA), 2017.

[2] C. Hachmann, G. Lammert, D. Lafferte, M. Braun: “Power System Restoration and Operation of Island Grids with Frequency Dependent Active Power Control of Distributed Generation”, NEIS 2017; Conference on Sustainable Energy Supply and Energy Storage Systems, Hamburg, Germany, 2017, pp. 1-6.

[3] IEEE PES Task Force on Microgrid Stability Analysis and Modeling: “Microgrid Stability Definitions, Analysis, and Modeling”, 2018.

[4] M. Shahabi, M. R. Haghifam, M. Mohamadian, and S. A. Nabavi-Niaki, “Microgrid Dynamic Performance Improvement Using a Doubly Fed Induction Wind Generator,” IEEE Trans. Energy Convers., vol. 24, no. 1, pp. 137–145, 2009.

[5] F. Hafiz and A. Abdennour, “Optimal use of kinetic energy for the inertial support from variable speed wind turbines,” Renewable Energy, vol. 80, pp. 629–643, 2015.

[6] J. Ekanayake and N. Jenkins, “Comparison of the Response of Doubly Fed and Fixed-Speed Induction Generator Wind Turbines to Changes in Network Frequency,” IEEE Trans. Energy Convers., vol. 19, no. 4, pp. 800–802, 2004.

[7] Technical requirements for the connection and operation of customer installations to the medium voltage network (TAR medium voltage), VDE-AR-N 4110, Nov., 2018.

[8] S. Heier, Grid integration of wind energy: Onshore and offshore conversion systems. Chichester, West Sussex, United Kindgom: Wiley, 2014.

[9] H. Laaksonen, D. Ishchenko, and A. Oudalov, "Adaptive Protection and Microgrid Control Design for Hailuoto Island," IEEE Trans. Smart Grid, vol. 5, no. 3, pp. 1486–1493, 2014.

[10] Y. A. Katsigiannis and E. S. Karapidakis, "Operation of wind-battery hybrid power stations in autonomous Greek islands," in 2017 52nd International Universities Power Engineering Conference (UPEC), Heraklion, Aug. 2017 - Aug. 2017, pp. 1–5.

[11] A. Roehder et al., "Transmission system stability assessment within an integrated grid development process", in CIGRE CSE, 2017.

[12] F. Milano: Power System Modelling and Scripting. Lonodon: Springer-Verlag, 2010.

[13] J. Machowski, J. Bialek, J. Bumby: Power System Dynamics: Stability and Control, 2008.

[14] IEEE Recommended Practice for Excitation System Models for Power System Stability Studies, IEEE Std 421.5-2016, Aug. 2016.

[15] P. Pourbeik et al., "Dynamic models for turbine-governors in power system studies," IEEE Task Force on Turbine-Governor Modeling, Jan. 2013.

[16] A. Perdana, "Dynamic models of wind turbines: A contribution towards the establishment of standardized models of wind turbines for power system stability studies," Ph.D. dissertation, Göteborg: Chalmers Univ. of Technology, 2008.

[17] I. Erlich, J. Fortmann, S. Engelhardt, J. Kretschmann: „Spannungsregelung mit moderner WEA-Technik", in Proc. 14. Kasseler Symposium Energie-Systemtechnik, pp. 108-117, Kassel, Germany, 2009.

[18] C. Cieslak, L. Grunwald: „Modelling Synthetic Inertia of Wind Turbines for Dynamic Power System Stability Studies," in 54th International Universities Power Engineering Conference (UPEC), Bucharest, Romania, Sept. 2019.

[19] G. C. Tarnowski, P. C. Kjar, P. E. Sorensen, and J. Ostergaard, "Variable speed wind turbines capability for temporary over-production," in *2009 IEEE Power & Energy Society General Meeting*, Calgary, AB, Canada, Jul. 2009, pp. 1–7.

[20] Strunz, K.; Abbasi, E.; Fletcher, R.; Hatziargyriou, N.D. Benchmark Systems for Network Integration of Renewable and Distributed Energy Resources; CIGRÉ TF C6.04.02, Technical Report 575; CIGRE: Paris, France, 2014.